[12] The isomer ratio was calculated by integration of the HPLC peaks corrected by the extinction coefficients. Remarkably, the equilibrium *cis*:*trans* ratio is slightly higher than for the azobenzene precursor **2** (90:10).
[13] Irradiation was performed in a spectrofluorometer (Fluromer-2; light source: 150 W xenon lamp; 5 nm path). At a concentration of 2 μM, isomer *trans*-**3** was obtained after 15 min.
[14] In the absence of visible light, the isomerization of *cis*-**3** to *trans*-**3** at 35 °C had a half-life of approximately 65 h.
[15] It should be borne in mind that *cis*-**3** is contaminated by 5% of the *trans* isomer.
[16] An azobenzene–peptide hybrid related to **3** but lacking the two glycines at the C terminus is unable to bind to the CREB site in either the *cis* or *trans* form (results not shown).
[17] The absence of specific binding was also corroborated by PAGE using ^{32}P end-labelled CREB18-half2 as the DNA probe.
[18] The UV spectrum of the peptide–DNA complex after 4 h irradiation with visible light is identical to that obtained before irradiation, suggesting that the *cis*-azobenzene unit was unable to switch to the *trans* form (see the Supporting Information).

TEM Studies of Platinum Nanowires Fabricated in Mesoporous Silica MCM-41**

Zheng Liu, Yasuhiro Sakamoto, Tetsu Ohsuna, Kenji Hiraga, Osamu Terasaki,* Chang Hyun Ko, Hyun June Shin, and Ryong Ryoo

Porous materials attract much attention as catalysts, catalyst supports, and shape/size-selective adsorbents, as well as containers for making new materials. According to the definition of IUPAC,[1] porous materials can be divided into three types according to their pore diameters: microporous (<2 nm), mesoporous (2–50 nm), and macroporous (>50 nm). Although zeolites, which belong to the microporous group, provide excellent catalytic properties as a result of their crystalline aluminosilicate networks, their applications are limited by the relatively small internal spaces and pore openings. Therefore, an expansion of the spaces is one of the main targets in the synthesis of porous materials.

In 1992, researchers at Mobil Corporation used a liquid crystal template to synthesize a new family of mesoporous silicates and aluminosilicates known as the M41S family.[2, 3] These ordered mesoporous materials have since attracted much attention. Silca MCM-41 is a member of the M41S family with a hexagonal array of one-dimensional pores. The diameter of the pores can be varied from 1.6 to 10 nm by using surfactants of different chain lengths or organic molecules for expanding the surfactant micelles.[4–11] Numerous studies have been reported on the synthesis of high-quality MCM-41, especially with pore diameters below 4.5 nm.[2–5, 12–14] Recently, the synthesis of very high quality MCM-41 was achieved by controlling the micelle packing parameter with two kinds of surfactant.[15] These MCM-41 molecular sieves attract considerable and growing attention because of their remarkable properties. The spaces of the mesoporous materials can be used as containers or templates for the synthesis of other new materials. Here we report on the structural characterization by transmission electron microscopy (TEM) and thermal stability of Pt nanowires as synthesized in the MCM-41 channels and of Pt nanowires removed from the silica template.

We synthesized MCM-41 silica by following a previously reported procedure;[15] platinum nanowires were prepared in the MCM-41 channels in a manner similar to that reported previously;[16] and unsupported Pt nanowires were obtained by removing the silica framework from the Pt/MCM-41 sample with an aqueous solution of hydrofluoric acid (see Experimental Section).

Figures 1 a and 1 b show high-resolution electron micoscopy (HREM) images of the calcined MCM-41 sample. Figure 1 a shows a uniform hexagonal arrangement of bright dots corresponding to the straight channels of MCM-41. The diffraction pattern in the inset of Figure 1 a clearly shows that the incident beam is along the [001] direction. The brightness and the shape of the channels seem to differ slightly from

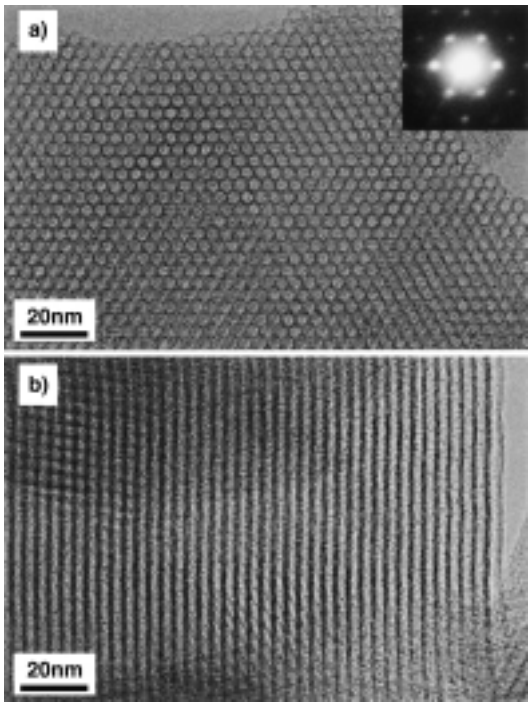

Figure 1. TEM images of calcined mesoporous MCM-41 along the channel direction (*c* axis; a) and perpendicular to it (b).

[*] Z. Liu
CREST, Japan Science and Technology Corporation
Tohoku University, Sendai 980-8578 (Japan)
O. Terasaki, Y. Sakamoto
Department of Physics
Graduate School of Science
Tohoku University
Sendai 980-8578 (Japan)
Fax: (+81) 022-217-6475
E-mail: terasaki@msp.phys.tohoku.ac.jp
T. Ohsuna, K. Hiraga
Institute for Materials Research
Tohoku University, 2-1-1 Katahira
Aoba-ku, Sendai 980-8577 (Japan)
C. H. Ko, H. J. Shin, R. Ryoo
Department of Chemistry and Center for Molecular Science
Korea Advanced Institute of Science and Technology
Taeduk Science Town
Taejon, 305-701 (Korea)

[**] A part of this work was supported by CREST, Japan Science and Technology Cooperation.

  1433-7851/00/3917-3107 $ 17.50+.50/0

place to place. This is a result of slight changes in diffraction conditions, which show a domain character. Note that all the HREM images are projected along the incident beam direction; therefore, the value of pore diameter from Figure 1a is the projection of the pores along the [001] direction and may be somewhat less than the actual value. Nevertheless, in principle, the pore diameter which is calculated from Figure 1b may give more reliable value than that obtained from other methods, on the assumption that the channels are cylindrical. The HREM method requires appropriate methods of data analysis to avoid artifacts that can lead to an incorrect result.[17, 18] The diameters of the channels are uniformly about 3.2 nm.

When Pt metal was supported on the MCM-41 silica, most of the Pt clusters were obtained in the form of nanowires. These nanowires followed the bending of the channels, although some Pt particles were observed on the external surfaces of the MCM-41 (Figure 2). The lengths of the Pt nanowires differed from place to place. The lengths ranged from several tens of nanometers to several hundreds of nanometers.

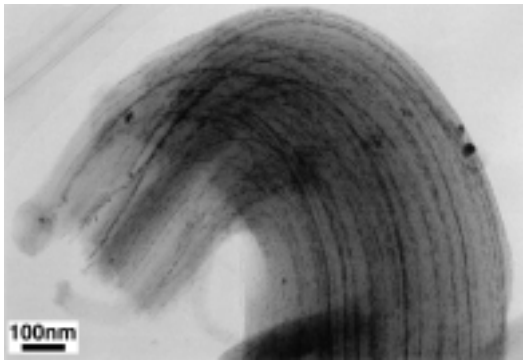

Figure 2. TEM image of Pt nanowires in the channels of calcined mesoporous MCM-41 (Pt/MCM-41).

Figure 3 shows an HREM image of Pt/MCM-41 taken in the [001] direction, which gives the cross-sections of the MCM-41 channels. The channels are parallel to the incident beams and arranged in a honeycomb fashion. Two different types of dark contrast from Pt particles are apparent. The smaller, darker areas correspond to Pt nanowires located inside the honeycomb channels. The others give a smeared contrast over the channels, which corresponds to a Pt particle on the external surface. They are indicated by small and large arrows, respectively. The result suggests that the Pt nanowires are well confined in the channels.

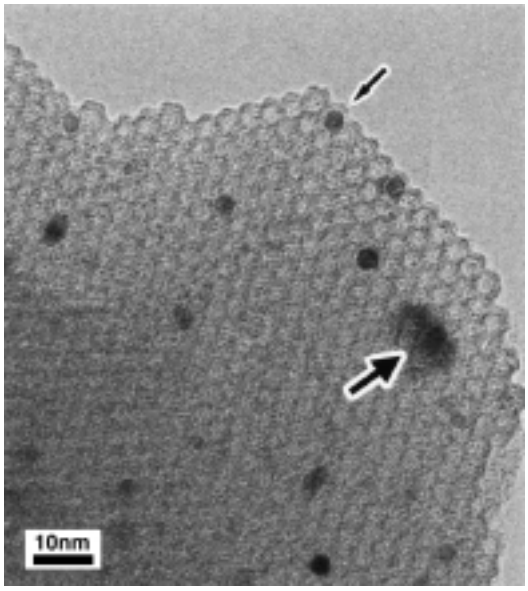

Figure 3. TEM image of a Pt/MCM-41 sample taken in the [001] direction.

Figures 4a and 4b show a low-magnification TEM image and an HREM image, respectively, of the Pt nanowires extracted from Pt/MCM-41 by dissolution of the silica frameworks with HF. The diameter of the Pt nanowires was

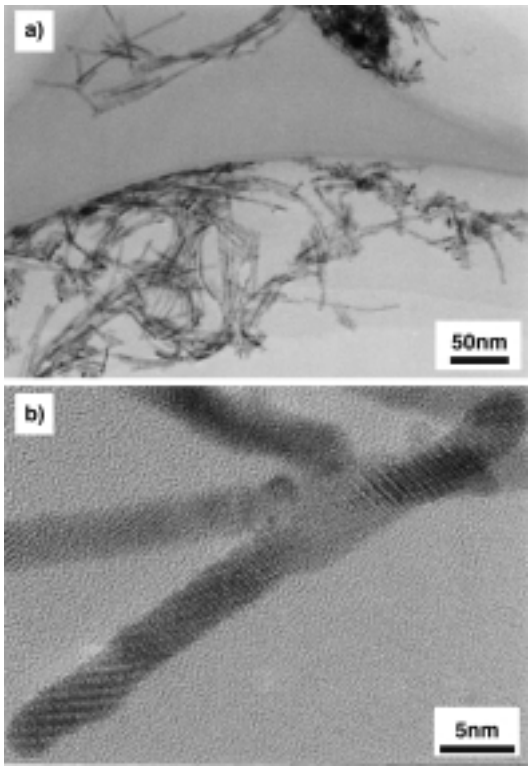

Figure 4. a) Low-magnification TEM image and b) HREM image of Pt nanowires extracted from the Pt/MCM-41 samples.

calculated from many HREM images that were similar to Figure 4b to be 3.0 nm. This is almost the same value as that of the channels. The Pt nanowires have good crystallinity, each can be regarded as a single crystal, and the wires have fairly smooth surfaces with specific indices (see below). It was reported that the shape of the pores of MCM-41 is hexagonal rather than circular.[19] However, it is difficult to discern whether the cross-section of the Pt nanowires is hexagonal or circular from Figures 3 and 4b.

To determine whether certain directions are preferred during the growth of Pt nanowires, we studied which planes of the Pt nanowires make contact with the channels. Figures 5a and 5b are typical HREM images of Pt nanowires showing the planes parallel to the channel walls. The insets are magnified images of the areas indicated by rectangles. The values of the *d* spacings between the planes shown in the images indicate that they are coincident with the {111} and {200} planes of Pt.

  1433-7851/00/3917-3108 $ 17.50+.50/0

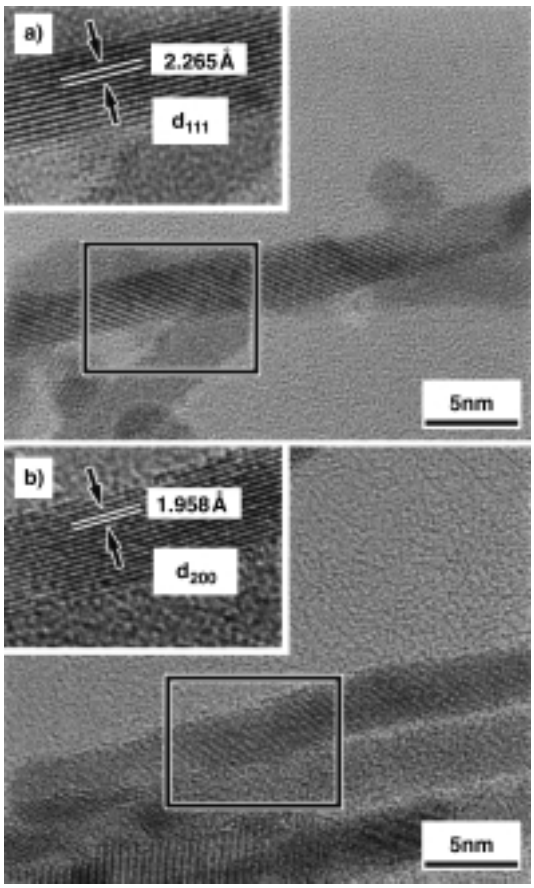

Figure 5. HREM images of Pt nanowires showing the planes parallel to the wall of channels. a) {111} planes; b) {200} planes.

Since the channels are not completely straight, steps are present on the atomic scale. Ignoring the inclination, it can be concluded that the indices of the planes that are parallel to the channel walls are {111} and {200} in Figures 5a and 5b, respectively. We can also deduce the same result from the other HREM images. Hence, the only possibilities for the indices of the planes parallel to channel walls are {111} and {200}. If the planes parallel to channel walls in one Pt nanowire are {111} and {200}, then the axis of preferential growth should contain both {111} and {200} planes. For platinum, which has a face-centered cubic structure, it can be concluded that the ⟨110⟩ axes are the preferential growth directions of the Pt nanowires.

From the viewpoint of synthesis and applications, the thermal stability of the Pt nanowires is important. Figure 6 shows a series of TEM images of the Pt/MCM-41 sample observed in situ by using heated-stage TEM. The Pt nanowires in the channels of MCM-41 were stable and remained unchanged up to 500 °C. The Pt nanowires did not agglomerate or diffuse to the outer surface.

The Pt nanowires that were extracted from the Pt/MCM-41 samples were also observed in situ by heated-stage TEM under the same condition as for the Pt/MCM-41 samples. Figure 7 shows the TEM images taken at various temperatures. The Pt nanowires began to agglomerate at around 300 °C and broke below 400 °C, as indicated by the arrows in Figure 7. Hence, the Pt nanowires in the channels of MCM-41 were much more stable than those outside the channels.

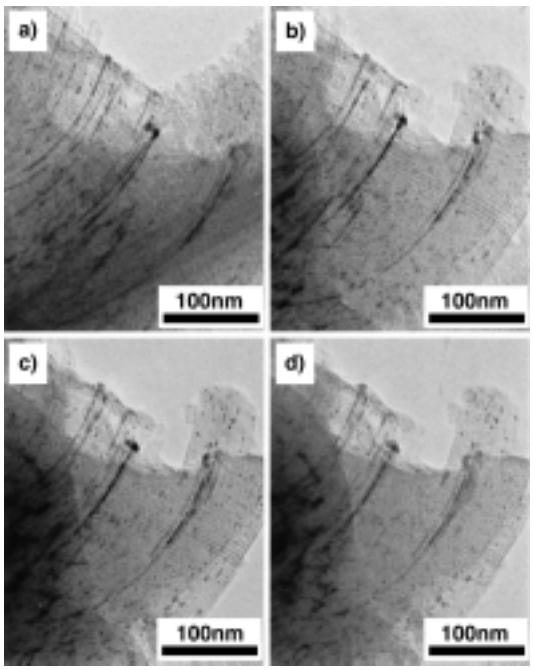

Figure 6. TEM images of a Pt/MCM-41 sample observed in situ by heated-stage TEM. a) Room temperature; b) 300 °C; c) 400 °C; d) 500 °C.

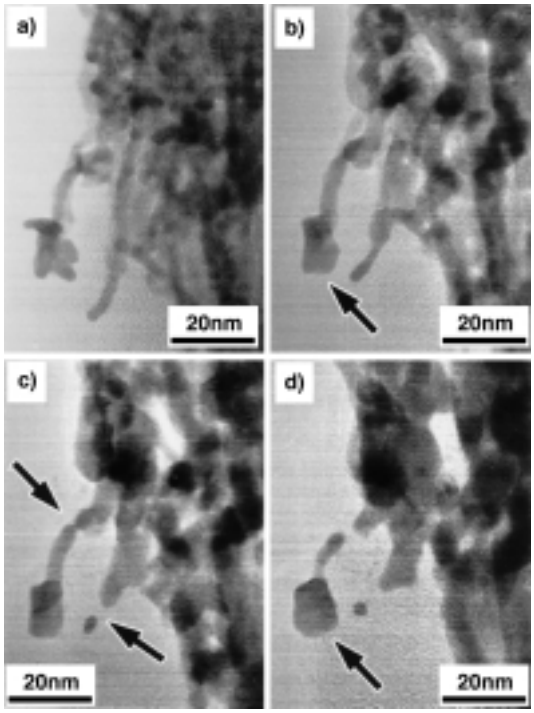

Figure 7. TEM images of Pt nanowires observed in situ by heated-stage TEM. a) Room temperature; b) 300 °C; c) 400 °C; d) 500 °C.

Experimental Section

MCM-41: An aqueous solution of sodium tetrasilicate (Si/Na = 2) was used as the silica source and added drop by drop to an aqueous solution of tetradecyltrimethylammonium bromide (TTMABr, Aldrich) surfactant at room temperature while the solution was stirred vigorously. After the mixture had been continuously stirring for 1 h, the resultant gel mixture was heated for 24 h at 100 °C. The molar composition of the gel mixture was 3.0 SiO_2:0.75 Na_2O:1.0 TTMABr:400 H_2O. The mixture was cooled to room temperature, and the pH was adjusted to 10 with acetic acid. The mixture

  1433-7851/00/3917-3109 $ 17.50+.50/0

was heated again for 48 h at 100 °C. The pH adjustment and subsequent heating were repeated, and the precipitated MCM-41 product was collected by filtration. The product was washed with EtOH/HCl and calcined in air at 550 °C.

Pt/MCM-41: The calcined MCM-41 sample was slurried in a 3×10^{-3} wt % aqueous solution of $[Pt(NH_3)_4](NO_3)_2$ (Aldrich) for 3 h at room temperature to incorporate $[Pt(NH_3)_4]^{2+}$ ions into the channels of MCM-41 by exploiting the weak ion-exchange capability of the silica material. The solution-to-silica ratio was 100 mL g^{-1}. After this treatment, the sample was collected by filtration and subsequently dried in a vacuum oven at room temperature. The ion-exchanged Pt precursor was activated while being slowly heated to 320 °C in a stream of O_2 and then reduced with a stream of H_2 at 300 °C. The resultant sample contained 0.1 wt % Pt seed. This sample was immersed in 1.5×10^{-1} wt % aqueous solution of $[Pt(NH_3)_4(NO_3)_2]$, which corresponded to 5 wt % of the MCM-41 silica on the basis of Pt. After the solvent was completely evaporated in a rotary evaporator, the sample was further dehydrated in a vacuum oven at room temperature. The impregnated Pt-metal precursor was finally reduced in a stream of H_2 while the temperature was increased from room temperature to 300 °C over 4 h and maintained at 300 °C for 2 h. These treatments gave Pt nanowires inside the MCM-41 channels.

Unsupported Pt nanowires: A small amount of Pt/MCM-41 was added to a 10 wt % aqueous solution of HF diluted with ethanol. The silica was completely dissolved after stirring this solution gently at room temperature. The Pt nanowires were collected by filtration, washed with ethanol, and stored in ethanol until used.

TEM measurements: All samples (calcined MCM-41, Pt/MCM-41 and extracted Pt nanowires) were suspended in ethanol (99.9 vol %) by ultrasonication. The suspension was deposited on a carbon microgrid for TEM observation. The HREM observations were performed with a 400 kV electron microscope (JEM-4000EX) at room temperature. High-temperature observations were carried out by 1250 kV EM (JEM-1250) with a top-entry high-temperature stage.

Received: April 6, 2000 [Z14950]

[1] K. S. W. Sing, D. H. Everett, R. H. W. Haul, L. Moscou, R. A. Pierotti, J. Rouquerol, T. Siemieniewska, *Pure Appl. Chem.* **1985**, *57*, 603.
[2] C. T. Kresge, M. E. Leonowicz, W. J. Roth, J. C. Vartuli, J. S. Beck, *Nature* **1992**, *359*, 710.
[3] J. S. Beck, J. C. Vartuli, W. J. Roth, M. E. Leonowicz, C. T. Kresge, K. D. Schmitt, C. T.-W. Chu, D. H. Olson, E. W. Sheppard, S. B. McCullen, J. B. Higgins, J. L. Schlenker, *J. Am. Chem. Soc.* **1992**, *114*, 10834.
[4] N. K. Raman, M. T. Anderson, C. J. Brinker, *Chem. Mater.* **1996**, *8*, 1682.
[5] A. Sayari, *Chem. Mater.* **1996**, *8*, 1840.
[6] C.-Y. Chen, S. L. Burkett, H.-X. Li, M. E. Davis, *Microporous Mater.* **1993**, *2*, 27.
[7] A. Monnier, F. Schuth, Q. Huo, D. Humar, D. I. Margolese, R. S. Maxwell, G. D. Stucky, M. Krishnamurty, P. Petroff, A. Firouzi, M. Janicke, B. F. Chmelka, *Science* **1993**, *261*, 1299.
[8] Q. Huo, D. I. Margolese, U. Ciesla, P. Feng, T. E. Gier, P. Sieger, R. Leon, P. M. Petroff, F. Shüth, G. D. Stucky, *Chem. Mater.* **1994**, *6*, 1176.
[9] P. T. Tanev, T. J. Pinnavaia, *Science* **1995**, *267*, 865.
[10] Q. Huo, D. I. Margolese, G. D. Stucky, *Chem. Mater.* **1996**, *8*, 1147.
[11] A. Sayari in *Recent Advances and New Horizons in Zeolite Science and Technology* (Eds.: H. Chon, S. I. Woo, S.-E. Park), Elsevier, Amsterdam, **1996**, p. 1.
[12] A. Sayari, *Stud. Surf. Sci. Catal.* **1996**, *102*, 1.
[13] A. Sayari, P. Liu, *Microporous Mater.* **1997**, *12*, 149.
[14] A. Corma, *Chem. Rev.* **1997**, *97*, 2373.
[15] R. Ryoo, C. H. Ko, I.-S. Park, *Chem. Commun.* **1999**, 1413 – 1414.
[16] C. H. Ko, R. Ryoo, *Chem. Commun.* **1996**, 2467 – 2468.
[17] S. Schacht, M. Janicke, F. Schuth, *Microporous Mesoporous Mater.* **1998**, *22*, 485.
[18] Y. Sakamoto, S. Inagaki, T. Ohsuna, N. Ohnishi, Y. Fukushima, Y. Nozue, O. Terasaki, *Microporous Mesoporous Mater.* **1998**, *21*, 589.
[19] M. Kruk, M. Jaroniec, Y. Sakamoto, O. Terasaki, R. Ryoo, C. H. Ko, *J. Phys. Chem. B.* **2000**, *104*, 292.

Network Polysilanes: Synthesis, Electrical Conductivity, Charge-Transfer Interaction, and Photoconductivity

Takanobu Kobayashi, Hirokazu Shimura, Shin Mitani, Saeko Mashimo, Aiko Amano, Toshihisa Takano, Minoru Abe, Hamao Watanabe,* Masashi Kijima, Hideki Shirakawa, and Hiroyuki Yamaguchi

Much attention has been paid to polysilanes because of their unique and versatile properties resulting from extensive delocalization of the σ electrons. These properties have made polysilanes useful as photoresists, ceramic precursors, photoconductors, semiconductors, and nonlinear optical materials in high technology fields.

With MeO-functionalized polysilanes as the starting material,[1] we recently obtained a new type of network polysilane, $[MeSi(OMe)_x(R)_y]_n$, with various R groups (alkyl, aralkyl, alkenyl, and aryl) as the side chains by the action of the corresponding Grignard reagents RMgX (X = Cl, Br).[2] Among these polysilanes, those having *N*,*N*-dialkylaminophenyl groups as side chains (*p*-$R'_2NC_6H_4$; R′ = Me, Et, Pr) exhibited electrical conductivities on the order of 10^{-3} S cm^{-1} upon iodine doping; they are essentially stable under oxidative conditions because of their network structures.[2] Although linear polysilanes generally show high hole mobility or photorecepting ability due to their electrical characteristics,[3, 4] no studies regarding such properties for network polysilanes have appeared so far. This led us to study network polysilanes for applications as conducting materials when combined with organic electron acceptors such as 9,10-dicyanoanthracene (DCA), *p*-chloranil, and tetracyanoquinodimethane (TCNQ).

Studies on the preparation and properties of network polysilanes arising from Wurtz-type coupling reactions with alkylated trichlorosilanes as starting materials have appeared,[5] whereas there are only limited reports on arylated network polysilanes, which are accessible using the corresponding trichlorosilanes.[6] As part of a continuing study on network polysilanes, we now report on the properties, charge-transfer interactions with organic electron acceptors, photocarrier generation as well as electrical conductivity of two types of network polysilanes. The network polysilanes were prepared by homo- or copolymerization using arylated

[*] Prof. Dr. H. Watanabe, T. Kobayashi, H. Shimura, S. Mitani, S. Mashimo, A. Amano, T. Takano, M. Abe
Department of Chemistry (Materials Science)
Faculty of Engineering, Gunma University
Gunma, Kiryu 376-8515 (Japan)
Fax: (+81) 277-30-1300
E-mail: hwatanab@chem.gunma-u.ac.jp
Prof. Dr. H. Shirakawa, Dr. M. Kijima
Institute of Materials, University of Tsukuba
Tsukuba, Ibaraki 305-8571 (Japan)
Dr. H. Yamaguchi
Department of Electronic Engineering, Gunma University
Gunma, Kiryu 376-8515 (Japan)

Supporting information for this article is available on the WWW under http://www.wiley-vch.de/home/angewandte/ or from the author.

  1433-7851/00/3917-3110 $ 17.50+.50/0